CAGRA+GR Campaign Experiments

The CAGRA+GR Collaboration

CAGRA+GR campaign experiments were performed at the Research Center for Nuclear Physics (RCNP) in October–December, 2016 (Fig. 1). CAGRA stands for Clover Array Gamma-ray spectrometer at RCNP/RIBF for Advanced research [1]. CAGRA was placed at the target position of the high-resolution spectrometer, Grand Raiden (GR), for high-resolution coincidence measurements with a particle spectrometer and a gamma-detector array. The campaign experiments aimed at studying the nature of the pygmy dipole resonances, isovector spin-flip responses of nuclei for astrophysical neutrino-nucleus inelastic-scattering, gamma-transitions in the super-deformed band-head, and excitation of high-spin states via light-ion reactions.

The idea of combining CAGRA and GR was first discussed during the Clover12 symposium held in Osaka in 2012. After the approval of the CAGRA project by the Physics-Program Advisory Committee (P-PAC) at RCNP, detailed experimental proposals were discussed in the CAGRA13 conference in Osaka in 2013. Sixteen abstracts were submitted to the CAGRA collaboration for the part of the CAGRA+GR campaign in the end of 2013. The collaboration later organized to combine the abstracts into groups of proposals with the help of the CAGRA board. Consequently, six proposals were submitted to the Beam-Program Advisory committee (B-PAC) in 2014-2016, and five proposals were approved as listed in Table 1.

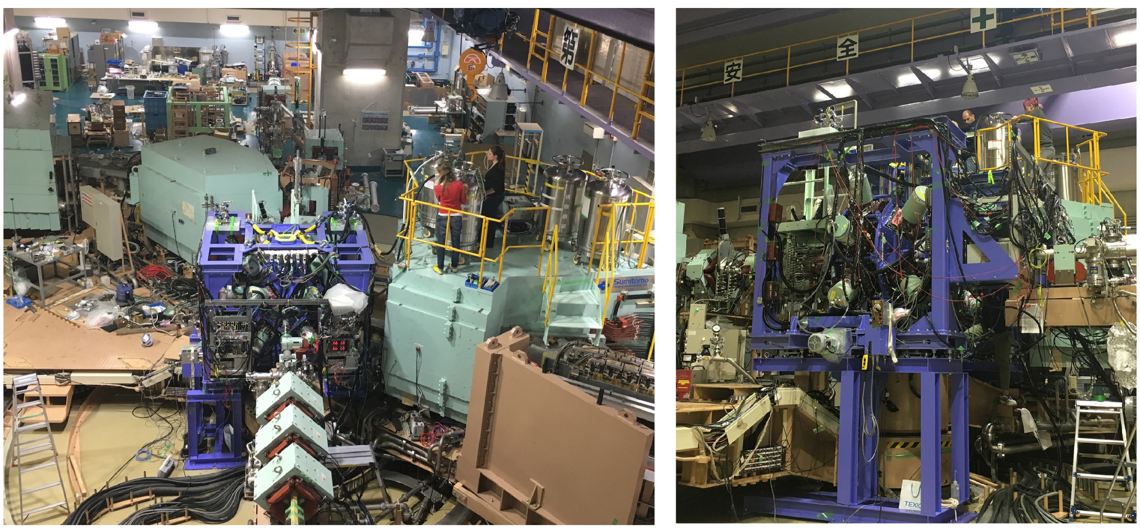

Figure 1: CAGRA placed at the target position of the Grand Raiden spectrometer with the GRAF beam line in the CAGRA+GR campaign in October-December 2016.

Table 1: List of the approved experiments of the CAGRA+GR campaign.

Exp. Number	Title	Beam time (days)	Ref.
E441	The (^{6}Li,^{6} Li$'$[3.56MeV]) reaction as a novel probe for studying the inelastic neutrino-nucleus response in astrophysical scenarios	5	[2]
E450	Study of the structure of the pygmy dipole resonance states via the $(p, p'\gamma)$ and $(\alpha, \alpha'\gamma)$ reactions	25	[3]
E454	Study of the Structure of the pygmy dipole resonance states in ^{64}Ni via the $(p, p'\gamma)$ and $(\alpha, \alpha'\gamma)$ reactions	6	[4]
E470	Search for superdeformed states in ^{28}Si via γ-particle coincidence measurements	6	[5]
E471	Study of high-spin state population by light-ion reactions	3	[6]

The design of the mechanical frame of CAGRA for the CAGRA+GR experiment started in January 2014 and finished in June 2016. The frame was manufactured in 2016. The frame was designed to be movable between the target position and the maintenance position by using a crane. CAGRA was placed at the maintenance position during the tuning of the primary beam to protect the crystals from charged particles and neutrons. The height of the legs of the frame is motor-adjustable for smooth landing of CAGRA from the crane. The frame could support sixteen detectors. We decided to place in total twelve clover detectors at 90 and 135 degree positions with respect to the beam direction, and four large-volume $LaBr_3$:Ce detectors (3.5"$\phi\times$8"L) [8] at 45 degree positions where higher rates of charged particles and neutrons were expected. The clover detectors were brought together from Argonne National Laboratory (ANL), Tohoku University, US Army Research Laboratory (ARL), and Institute of Modern Physics (IMP). The $LaBr_3$:Ce detectors were from INFN sezione di Milano. BGO Compton-suppression shields from ANL were used for ANL and ARL clovers. The detailed configuration is described in another article in this annual report [7]. The bottom two detectors at the 90 deg. position were fixed to the CAGRA frame while the other detectors were fixed on two hemisphere frames (left and right from the beam direction). Each hemisphere frame could be horizontally retracted from the target center on linear guides on the CAGRA frame.

To realize low-background gamma-ray detection at the target position in coincidence with light ions scattered at forward angles, we combined CAGRA with the Grand RAiden Forward mode (GRAF) beam line. At the GRAF beam line, which allows setting of GR at 4.5-19.0 degrees, the primary beam is transported from the target to a well-shielded beam dump placed in a wall at 25 meters downstream of the target. The beam line was proposed in December 2012 and the construction was completed in March 2014.

The target chamber was made of aluminum pipes with a thickness of 3 mm. The outer diameter of the pipe for the beam transport (target ladder) was 90 (80) mm. The target frames and the target ladder were also made of aluminum. The target was tilted by 22.5 degrees from the perpendicular position to the beam direction in order to minimize the material between the target and the crystals. Vacuum adapters between GR and the target chamber were prepared for each of the GR angles of 0.0, 4.5, 5.5, 6.8, 9.1, and 11.4 degrees

Six commissioning experiments were performed from May 2014 to June 2016 including two as parasite of other physics measurements. The experiments aimed at testing the background condition such as neutron fluence around the target, background spectra of the HPGe and LaBr3 detectors, neutron damage of the HPGe detectors, and the performance of the trigger, the data acquisition (DAQ) system and the analyzer under various combinations of beams and targets.

The experimental setup of the CAGRA+GR campaign started in June 2016. At first, the standard scattering chamber was removed. Then, the quadrupole magnet of the large-acceptance spectrometer (LAS) was removed together with the vacuum chamber, the entrance gate valve, and the slit box of the LAS. The WS beam line was rearranged to the GRAF mode. The base structure of CAGRA was placed at the target position. The maintenance dock and the DAQ system of CAGRA were placed at the north side of the beam line before the target. Performance of each detector was tested before mounting on CAGRA. Noise conditions of the detectors were investigated on and off the CAGRA frame. Finally, all the detectors were mounted on the CAGRA frame in the end of September 2016.

The campaign experiments were separated into four parts: I) an alpha beam at 130 MeV from October 3rd to 26th, II) a proton beam at 80 MeV from November 11th to 16th, III) a proton beam at 295 MeV from December 4th to 9th, and IV) a ^{6}Li beam at 600 and 130 MeV from December 13th to 21st. The typical parameters of the measurements are summarized in Table 2.

The beams were transported in the achromatic mode, *i.e.* without making the dispersion matching, in order to prevent the beam halo from hitting the beam pipe and thus producing background in CAGRA. Liquid nitrogen was filled to the clover detectors twice a day throughout the campaign except during the annealing process described below. For each of the beam times, CAGRA was placed at the maintenance position in the beginning during the beam tuning. CAGRA was moved to the target position after achieving a good beam on target and the GR parameters were optimized. Moving CAGRA to the target position took 3 hours. Beam intensity was optimized to have an individual rate of $\sim$10 (20) kHz for ANL (IMP) clover crystals depending on the type of the beam and target.

The CAGRA data were taken using the digitizer and trigger modules developed for GRETINA [9] with firmware and DAQ developed for Digital Gammapshere [10]. The GR data were taken by the standard GR-DAQ system. A VME module, MyRIAD developed at Argonne National Laboratory, was added in the GR-DAQ to record the timestamp of each event and to distribute the GR trigger to the CAGRA-DAQ. The CAGRA data were taken only in coincidence with the GR trigger while the GR data were taken for every GR trigger independently of the gamma detectors. Online event-building and analysis was done by using the GRUTinizer package [11].

The neutron fluence was monitored by counting the ^{72}Ge(n,n') peak at 693.4 keV in order to estimate the radiation damage of the clover crystals. Here, we adopted the approximate reaction between the neutron fluence and the detected peak counts suggested by Bell as shown below [12]

$$\frac{\text{neutrons}}{\text{cm}^2} = \frac{300 \times \text{counts in 693.4 keV peak}}{\text{detector volume in cm}^3}\,. \quad (1)$$

Table 2: Parameters of the measured reactions.

	Beam and Energy (MeV)	Target Nucleus	GR Angle (deg)	Targe Thickness (mg/cm^2)	Beam Intensity (enA)	Beam Charge (μC)
I)	α 130	^{90}Zr	4.5	1.95	1-10	1,020
		^{94}Zr	4.5	4.0	1-6	404
		^{64}Ni	4.5	3.55	9	1,610
		^{120}Sn	4.5	2.7	4-5	1,106
		^{206}Pb	4.5	1.3	15	3,930
		^{208}Pb	4.5	2.03	2-10	140
		^{nat}Si	9.1	11	3	1,250
II)	p 80	^{208}Pb	4.5, 6.6, 8.8, 11.2	2.03	10-15	3,950
		^{90}Zr	6.6	1.95	4-10	850
		^{94}Zr	6.6	4.0	4	390
		^{124}Sn	6.6	4.0	4	540
		^{206}Pb	6.6	1.3	13	1,440
				Annealing		
III)	p 295	^{64}Ni	0.0	3.55	2.5	510
IV)	^{6}Li 600	^{nat}C	0.0	15.2	0.1-0.2	13
		^{24}Mg	0.0	9.8	1	42
		^{56}Fe	0.0	10.2	1	39
		^{93}Nb	0.0	10.1	1	73
		^{40}Ca	11.2	1.6	10	530
	^{6}Li 130	^{40}Ca	11.2	1.6	10	690
				Annealing		

The neutron fluence was kept well below 4×10^9 neutrons/cm^2 until the annealing of the crystals. The number is the practical limit for "light damage" suggested by Bell. For example, the monitored neutron fluence was 4×10^8 neutrons/cm^2 in the first beam time of an α beam at 130 MeV and 6×10^7 in the ^{208}Pb$(p, p'\gamma)$ measurement during the second beam time with a proton beam at 80 MeV. The resolution of a crystal of an ANL clover placed at 90 deg was 2.0 keV at $E_\gamma = 1.33$ MeV before starting the campaign. It deteriorated to 4.4 keV at the end of the second beam time. The peak shape showed a low energy tail which is typical after neutron irradiation. All the used clovers were annealed at a temperature of 85 °C for 96 hours by using the pre-mounted heater coil and the Pt100 temperature monitor. The photo-peak of the crystals recovered to the original width with a Gaussian shape. The clover detectors were annealed again after the fourth beam time.

The typical ranges of the measured excitation-energy were 2.5–14.5 MeV for E_α=130 MeV, 5.5–12.5 or 1.5–8.5 MeV for E_p=80 MeV, and 4–26 MeV for E_p=295 MeV. A spectrum of the ^{64}Ni(p, p') reaction at E_p=295 MeV is shown in the left panel of Fig. 2. The excitation energy resolution was 110 keV. The Giant Dipole Resonance (GDR) is clearly observed as a big bump with the center at 16.5 MeV. A concentration of the strengths at 7-11 MeV on the lower energy tail of the GDR consists of the Pygmy Dipole Resonance (PDR) and the spin-$M1$ excitations. A particle-gamma coincidence spectrum is shown in the right panel of Fig. 2 for the same reaction. The vertical axis is the energy deposit of gamma rays in the LaBr$_3$ detectors. The direct gamma-decay to the ground state is observed as a band close to the X=Y line. Below the neutron separation energy of S_n=9.66 MeV, cascade gamma decays are also observed. Above S_n, gamma-decays after the neutron decay are observed. The sharp peak at 15.62 MeV corresponds to the T-upper (T=5) 1^+ state, from which neutron decay is forbidden due to the isospin conservation [13]. Its strong gamma-decay is observed in the two-dimensional histogram. A particle-gamma coincidence spectrum with the clover detectors is shown in another article of this annual report [14].

The campaign experiments have been successfully performed with the participation of 60 collaborators. Among them 42 collaborators came from 9 countries and 15 institutions from outside Japan. More than 90 people contributed to the campaign including the preparation stage of the proposals and during the commissioning experiments.

We appreciate the invaluable support from RCNP for realizing the campaign experiments. We are indebted to the cyclotron accelerator group and the operators for providing the excellent beams. We thank the technical staff of RCNP for designing the CAGRA frame and for preparing the infrastructures. Finally, we gratefully acknowledge the CAGRA board members.

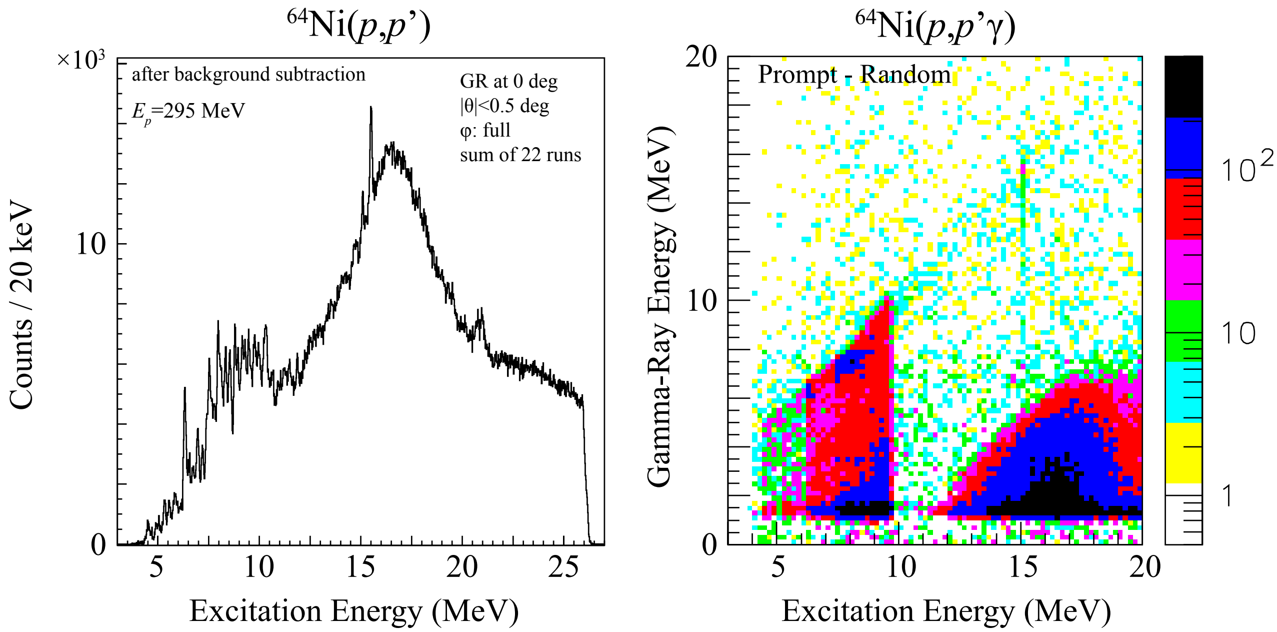

Figure 2: Sample spectra of the ^{64}Ni$(p, p'\gamma)$ reaction at E_p=295 MeV and at zero degrees. Left: excitation energy spectrum measured by the Grand Raiden spectrometer. Right: coincidence spectrum of the gamma-ray energy detected by the LaBr3 detectors versus the excitation energy. The energy calibration is very preliminary.

References

[1] E. Ideguchi, M. Carpenter, *et al.*, http://www.rcnp.osaka-u.ac.jp/Divisions/np1-a/CAGRA/index.html .

[2] RCNP Proposal E441 by S. Noji and R.G.T. Zegers.

[3] RCNP Proposal E450 by (1) A. Bracco, F. Crespi and N. Pietralla, (2) A. Zilges, V. Derya, D. Savran, M.N. Harakeh, P. von Neumann-Cosel, N. Pietralla and V. Werner (3) D. Savran, A. Zilges, V. Derya, M.N. Harakeh, P. von Neumann-Cosel, N. Pietralla and V. Werner, and (4) C. Iwamoto, A. Tamii, T. Hashimoto and P. von Neumann-Cosel.

[4] RCNP Proposal E454 by D. Savran and A. Zilges.

[5] RCNP Proposal E470 by D.G. Jenkins and D. Montanari.

[6] RCNP Proposal E471 by E. Ideguchi and A. Tamii.

[7] N. Kobayashi *et al.*, RCNP Annual Report 2016.

[8] A. Giaz *et al.*, Nucl. Instrum. Meth. Phys. Res. A **729**, 910 (2013).

[9] J. Anderson *et al.*, 2009 IEEE Transactions on Nuclear Science **56**, 258 (2009).

[10] J. T. Anderson *et al.*, IEEE Nuclear Science Symposium and Medical Imaging Conference (NSS/MIC), 1536 (2012).

[11] CAGRA-GrandRaiden/GRUTinizer, https://doi.org/10.5281/zenodo.571208 .

[12] G.F. Knoll "Radiation detection and measurement" 4th Edition' (Wiley, New Jersey, 2010); R.A.I. Bell, "Tables for Calibration of Radiation Detectors", Australian National Univ. Rep. ANU-P/606 (1974).

[13] N. Marty *et al.*, Nucl. Phys. A **396**, 145c (1983).

[14] J. Isaak *et al.*, RCNP Annual Report 2016.